

## ORIGINAL ARTICLE

JRK is a positive regulator of  $\beta$ -catenin transcriptional activity commonly overexpressed in colon, breast and ovarian cancerL Pangon<sup>1,2,7</sup>, I Ng<sup>1,7</sup>, M Giry-Laterriere<sup>1</sup>, N Currey<sup>1</sup>, A Morgan<sup>1</sup>, F Benthani<sup>1,2</sup>, PN Tran<sup>1</sup>, S Al-Sohaily<sup>1</sup>, E Segelov<sup>2</sup>, BL Parker<sup>3,4</sup>, MJ Cowley<sup>1,2,5</sup>, DC Wright<sup>6</sup>, L St Heaps<sup>6</sup>, L Carey<sup>6</sup>, I Rومان<sup>1,2</sup> and MRJ Kohonen-Corish<sup>1,2</sup>

The loss of  $\beta$ -catenin inhibitory components is a well-established mechanism of carcinogenesis but  $\beta$ -catenin hyperactivity can also be enhanced through its coactivators. Here we first interrogated a highly validated genomic screen and the largest repository of cancer genomics data and identified *JRK* as a potential new oncogene and therapeutic target of the  $\beta$ -catenin pathway. We proceeded to validate the oncogenic role of *JRK* in colon cancer cells and primary tumors. Consistent with a  $\beta$ -catenin activator function, depletion of *JRK* in several cancer cell lines repressed  $\beta$ -catenin transcriptional activity and reduced cell proliferation. Importantly, *JRK* expression was aberrantly elevated in 21% of colorectal cancers, 15% of breast and ovarian cancers and was associated with increased expression of  $\beta$ -catenin target genes and increased cell proliferation. This study shows that *JRK* is required for  $\beta$ -catenin hyperactivity regardless of the adenomatous polyposis coli/ $\beta$ -catenin mutation status and targeting *JRK* presents new opportunities for therapeutic intervention in cancer.

*Oncogene* (2016) 35, 2834–2841; doi:10.1038/onc.2015.347; published online 12 October 2015

## INTRODUCTION

Constitutive activation of Wnt/ $\beta$ -catenin signaling is a key oncogenic mechanism in several types of cancer. A broad range of mutations or gene alterations have been identified that cause upregulation of  $\beta$ -catenin activity.<sup>1</sup> However, in colorectal cancer *adenomatous polyposis coli* (*APC*) mutations are overly represented with 80% of colorectal cancers harboring *APC* mutations. Following *APC* mutation,  $\beta$ -catenin accumulates in the cytoplasm and in the nucleus leading to aberrant  $\beta$ -catenin-mediated transcription. Nuclear  $\beta$ -catenin stimulates gene transcription by recruiting chromatin-remodeling complexes and coactivators, such as BCL9 and Pygopus (PYGO) protein families.<sup>2</sup> Importantly, several studies are now showing that strategies aimed at blocking these coactivators could provide potent anti-tumoral effects.<sup>3</sup> The aim of this study was to identify novel proteins that are required for  $\beta$ -catenin oncogenic activity and to evaluate their potential therapeutic value.

Our work builds on data from a highly validated whole-genome siRNA screen that identified 33 genes that are required for efficient  $\beta$ -catenin transcriptional activity.<sup>4</sup> Importantly, this screen was performed using DLD1 and SW480, two *APC*-mutated cell lines, suggesting that inhibition of these genes could repress oncogenic  $\beta$ -catenin activity in tumors regardless of the *APC* mutation status. We hypothesized that opposite to the  $\beta$ -catenin repressive effect observed following knockdown, overexpression of these genes in cancer could be oncogenic. Using The Cancer Genomics Atlas (TCGA), the largest repository of cancer genomics data, we identified *JRK* to be commonly overexpressed in colon, breast and ovarian cancer.

*JRK* is the homolog of Earthbound (Ebd1) that was identified in *Drosophila* as an essential component of the Wnt/ $\beta$ -catenin signaling pathway.<sup>5</sup> It belongs to a family of proteins that contain centromere protein B-type DNA-binding domains. *JRK* protein interacts directly with the  $\beta$ -catenin transcriptional complex, including  $\beta$ -catenin itself, LEF1 and PYGO2. The binding of *JRK* to this complex is expected to stabilize the  $\beta$ -catenin/TCF complex, and facilitate recruitment of  $\beta$ -catenin to chromatin.<sup>5</sup> Thus *JRK* is functioning at the core of the  $\beta$ -catenin pathway and downstream of the APC-GSK3-AXIN destruction complex, making it an attractive therapeutic target.

In humans, germline *JRK* alteration has been implicated in juvenile myoclonic epilepsy,<sup>6</sup> but remarkably there are no previous studies addressing the expression of *JRK* in cancer or its functional significance in carcinogenesis. Here, we show that *JRK* upregulates  $\beta$ -catenin activity and is a potential therapeutic target regardless of the mutational status of the Wnt/ $\beta$ -catenin pathway.

## RESULTS

*In silico* analyses identify *JRK* as a potential new oncogene in colon, breast and ovarian cancer

We first hypothesized that genes located in regions of recurrent genomic amplification or showing overexpression in cancer present potential oncogenic activity. We determined the expression and gene copy number of 33  $\beta$ -catenin coactivator genes<sup>4</sup> using TCGA, the largest and most comprehensive set of cancer genome data.<sup>7,8</sup> We identified *JRK* as the only one of these genes that was overexpressed in three major cancer types: breast, colon

<sup>1</sup>The Kinghorn Cancer Centre, Garvan Institute of Medical Research, Darlinghurst, Sydney, New South Wales, Australia; <sup>2</sup>St Vincent's Clinical School, UNSW Medicine, UNSW Australia, Sydney, New South Wales, Australia; <sup>3</sup>Biological Mass Spectrometry Unit, Garvan Institute of Medical Research, Darlinghurst, Sydney, New South Wales, Australia; <sup>4</sup>Charles Perkins Centre, School of Molecular Bioscience, The University of Sydney, Sydney, New South Wales, Australia; <sup>5</sup>Kinghorn Centre for Clinical Genomics, Garvan Institute of Medical Research, Darlinghurst, Sydney, New South Wales, Australia and <sup>6</sup>Cytogenetics, The Children's Hospital at Westmead, Westmead, New South Wales, Australia. Correspondence: Dr L Pangon, Cancer Division, Garvan Institute of Medical Research, 384 Victoria St, Darlinghurst, Sydney, New South Wales 2010, Australia. E-mail: l.pangon@garvan.org.au

<sup>7</sup>These authors contributed equally to this work.

Received 22 December 2014; revised 22 May 2015; accepted 24 July 2015; published online 12 October 2015

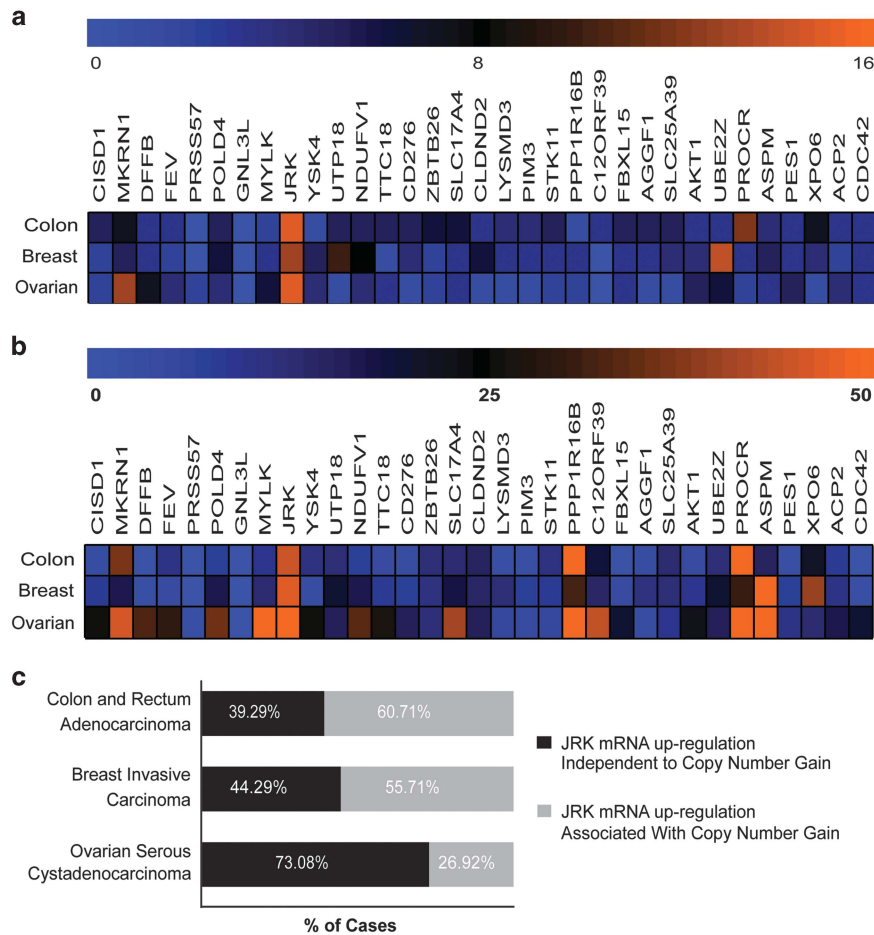


**Figure 1.** *In silico* analysis of TCGA data identify JRK as a potential new oncogene in colon, breast and ovarian cancer. **(a)** Heat map showing the percentage of tumors with mRNA upregulated by more than twofold for 33 potential  $\beta$ -catenin activators in breast, colon and ovarian cancer. JRK is overexpressed by more than twofold in 14.6% of breast invasive carcinoma, 16% colon and rectum adenocarcinoma, and 15.2% of ovarian serous cystadenocarcinoma. Data were obtained from cBioportal<sup>7,8</sup> (TCGA, all complete tumors); colon and rectum adenocarcinoma,<sup>26</sup> breast invasive carcinoma,<sup>27</sup> ovarian serous cystadenocarcinoma.<sup>28</sup> **(b)** Heat map showing the percentage of tumors with gene copy-number gain for 33 potential  $\beta$ -catenin activators in breast, colon and ovarian cancer. JRK gene copy-number gain is observed in 47% of breast invasive carcinoma, 45% colon and rectum adenocarcinoma, 53% ovarian serous cystadenocarcinoma. **(c)** JRK mRNA upregulation is independent of JRK copy-number gain in 39.29% of colon and rectum adenocarcinoma ( $n = 243$ ), 44.29% of breast invasive carcinoma ( $n = 842$ ) and 73.08% of ovarian serous cystadenocarcinoma ( $n = 261$ ).

and ovarian (Figure 1a). JRK is overexpressed by more than twofold in 16% of colon or rectum adenocarcinoma ( $n = 244$ ), 14.6% of breast invasive carcinoma ( $n = 774$ ), 35% of basal breast cancer ( $n = 81$ ) and 15.2% of ovarian serous cystadenocarcinoma ( $n = 316$ ).

JRK is located on chromosome 8q24, which is the most frequently amplified region across human cancer.<sup>9</sup> Consistent with its genomic location JRK is also commonly amplified in all three cancer types analyzed (Figure 1b). A prominent resident of chromosome 8q24 is the MYC proto-oncogene, raising the possibility that JRK overexpression could be a by-product of MYC amplification. We next analyzed the relation between JRK copy-number alterations, MYC copy-number alterations and JRK gene expression. As expected from their relative genomic proximity, increased JRK gene copy number was tightly associated with MYC gene copy number (>95% of JRK copy-number gain is associated with MYC copy-number gain in these cancers). However, a large proportion of cancers showing increased expression of JRK occurred independently of MYC or JRK gene copy-number gain in colon (39%), breast (44%) or ovarian cancers (73%; Figure 1c).

JRK is required for efficient transcription of endogenous  $\beta$ -catenin target genes across several cancer cell lines

To aid in the identification of a suitable model system for the assessment of JRK function, we quantified the expression of JRK by quantitative PCR (qPCR) in 56 cell lines (Supplementary Figure 1A). Both basal and luminal breast cancer cell lines showed statistically significant increased expression of JRK compared with normal breast cell lines (Supplementary Figure 1B).

We next tested the effect of JRK knockdown on  $\beta$ -catenin transcriptional activity in HCT15 and SW480 cell lines, that are both APC mutated. Remarkably, despite the modest reduction in JRK mRNA level (~40%), we observed a pronounced reduction in  $\beta$ -catenin transcriptional activity, as measured by the TOPFlash luciferase reporter in both cell lines (Figure 2a). We next determined the effect of JRK knockdown on the expression of several endogenous  $\beta$ -catenin target genes. JRK knockdown significantly reduced the expression of seven out of seven  $\beta$ -catenin target genes in HCT15 cells (Figure 2b) and three out of seven genes in SW480 cells (Figure 2c). To avoid possible small interfering RNA (siRNA) off-target effects we engineered two stable knockdown cell lines; HCT15 and RKO using two

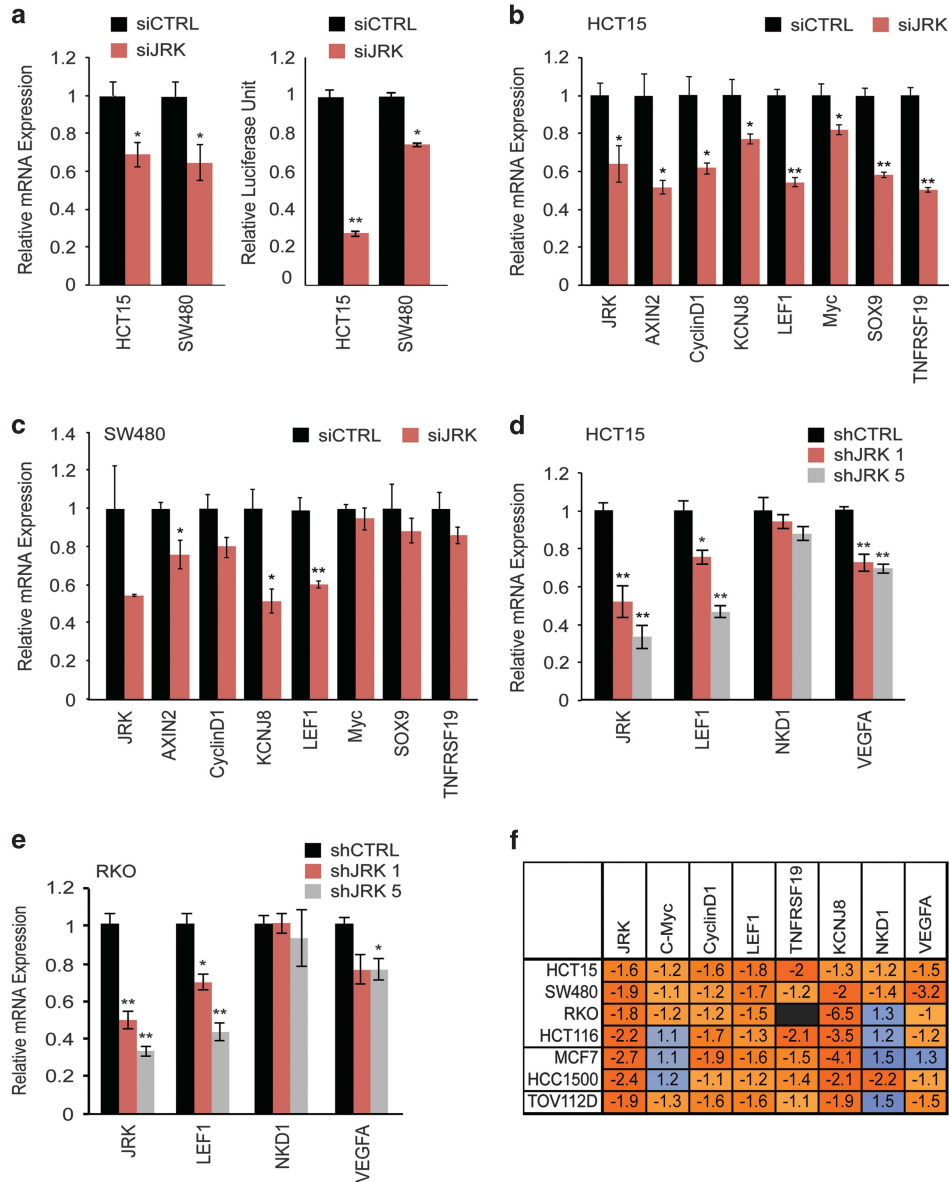


**Figure 2.** JRK is required for efficient transcription of endogenous  $\beta$ -catenin target genes across several cancer cell lines. **(a)** *JRK* knockdown represses  $\beta$ -catenin transcriptional activity as measured by the TOPFlash luciferase assay. HCT15 or SW480 cells were transiently transfected with *JRK* siRNA or control siRNA (siCTRL) with 1  $\mu$ g of the  $\beta$ -cat/TCF/LEF reporter construct. The y axis shows normalized relative luciferase activity, data are represented as mean s.d.,  $n=3$ . qPCR was used to confirm *JRK* knockdown in HCT15 and SW480. **(b, c)** *JRK* transient knockdown represses  $\beta$ -catenin target genes expression in HCT15 and SW480, respectively. *JRK* was transiently knocked down for 48 h and mRNA expression of  $\beta$ -catenin target genes was assessed by qPCR. Following *JRK* knockdown, seven and three target genes were showing significant reduction in mRNA level in HCT15 and SW480 cell lines, respectively. **(d, e)** *JRK* stable knockdown represses endogenous  $\beta$ -catenin target gene expression in HCT15 and RKO, respectively. Two Independent shRNAs (shJRK1 and shJRK5) were used to stably knockdown the expression of *JRK* in HCT15 and RKO cell lines. qPCR was used to assess three  $\beta$ -catenin target genes. **(f)** Effect of transient *JRK* knockdown on  $\beta$ -catenin target genes on two breast cancer cell lines (MCF7 and HCC1500), one ovarian cancer cell line (TOV112D) and four colorectal cancer cell lines (HCT15, SW480, HCT116 and RKO). Values shown are the fold change relative to control siRNA.

independent *JRK*-shRNAs (small hairpin RNAs). Following stable integration we confirmed the repressive effect of *JRK* knockdown on two out of three selected  $\beta$ -catenin target genes, *LEF1* and *VEGFA* in both cell lines (Figures 2d and e).

Finally, TCGA data show that, *JRK* is also overexpressed in breast and ovarian cancers (Figure 1a). We next tested the effect of transient *JRK* knockdown on seven  $\beta$ -catenin target genes in two breast cancer cell lines (MCF7 and HCC1500), one ovarian cancer cell line (TOV112D) and four colorectal cancer cell lines (HCT15, SW480, HCT116 and RKO). At least four out of the seven genes tested showed reduced expression following *JRK* knockdown in all

seven cell lines tested (Figure 2f). Further analysis of TCGA data also showed tendency towards co-occurrence for overexpression of *JRK* and nine  $\beta$ -catenin target genes in colon, breast or ovarian tumors (Supplementary Figure 2).

*JRK* is overexpressed in 21% of colon cancers compared with adjacent normal tissue and *JRK* expression is significantly associated with an increase in  $\beta$ -catenin target gene expression and  $\beta$ -catenin nuclear localization

To validate the TCGA data we determined *JRK* expression in a cohort of 130 primary colorectal cancers by qPCR. We found *JRK*

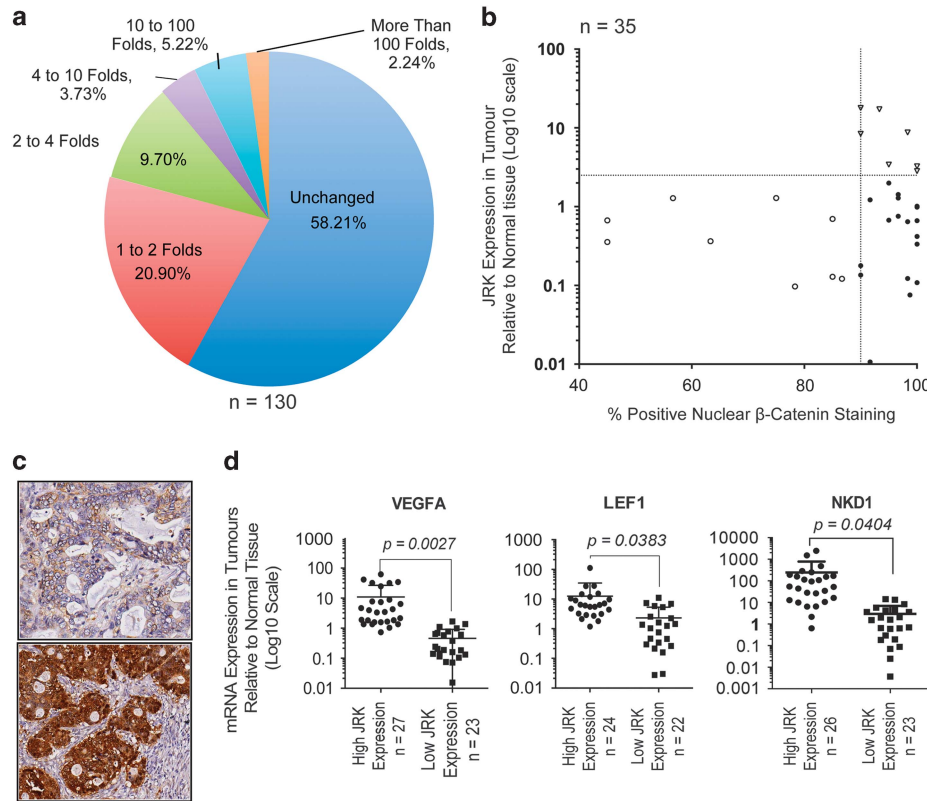


**Figure 3.** JRK is commonly overexpressed in colon cancer and associated with increased  $\beta$ -catenin target genes expression and increased  $\beta$ -catenin nuclear localization. **(a)** JRK is overexpressed by more than twofold in 21% of primary colon cancer. qPCR was performed on 130 primary colon cancers and 130 matched normal tissues. JRK mRNA expression varies greatly in the overexpressed group, with 7.5% showing an increase of  $>10$ -fold compared with normal matched tissue. **(b)** Tumors with high JRK expression show increased  $\beta$ -catenin nuclear staining, Fisher exact-test,  $P=0.038$ . Thirty-five primary tumors out of the 130 were stained for  $\beta$ -catenin and  $\beta$ -catenin nuclear staining was scored. Graph shows JRK expression in tumors relative to normal tissues and the percentage of positive nuclear  $\beta$ -catenin staining. **(c)** Representative immunohistochemistry staining of primary colon cancer showing  $\beta$ -catenin expression in a low JRK-expressing tumor (Top) and in a high JRK-expressing tumor (bottom). **(d)** Tumors with high JRK expression ( $n=24$ - $27$ ) are associated with increased expression of  $\beta$ -catenin target genes compared with low expressing tumors ( $n=22$ - $23$ ). *VEGFA*, *LEF1* and *NKD1* mRNA level were assessed by qPCR.

overexpressed by more than twofold in 21% of tumors compared with adjacent normal matched tissue (Figure 3a). We also observed 7.5% of tumors having  $>10$ -fold increased expression compared with normal.

In *Drosophila*, JRK was shown to be a component of the  $\beta$ -catenin transcriptional complex, binding to  $\beta$ -catenin, LEF1 and PYGO.<sup>5</sup> This study also suggested that JRK binds and stabilizes  $\beta$ -catenin in the nucleus. We next performed immunohistochemistry for  $\beta$ -catenin on 35 tumors and their matched control tissues. Tumors with high JRK expression ( $>2.5$ -fold) showed significantly higher nuclear  $\beta$ -catenin staining (Figures 3b and c).

We next determined the expression of three of the upregulated  $\beta$ -catenin target genes *LEF1*, *VEGFA* and *NKD1*, between the 30 lowest JRK-expressing colorectal tumors and 30 highest expressing JRK tumors. High JRK expression was significantly associated with an increased expression of these target genes compared with low JRK-expressing tumors (Figure 3d).

The N-terminal domain of JRK is required to promote cell proliferation

Increase in  $\beta$ -catenin activity is commonly associated with an increase in cell proliferation. To investigate the involvement of JRK on cell proliferation, we knocked down *JRK* in HCT116 colon cancer cells using lentivirus. Loss of *JRK* expression in two independent HCT116 clones resulted in a decrease in cell proliferation compared with control (Figure 4a). Conversely, stable

expression of JRK wild type in SW480 cell promoted cell proliferation (Figure 4b). We repeated the proliferation assay using SW480 stably expressing JRK( $\Delta$ N49), an N-terminal deletion that is known to impair JRK binding to  $\beta$ -catenin.<sup>5</sup> JRK( $\Delta$ N49) expression in SW480 cells failed to promote cell proliferation (Figure 4b).

Finally, consistent with its transcriptional coactivator role, we found JRK-WT to be predominantly localized in the nucleus forming a large number of small nuclear foci and a few large foci (Figure 4c). Conversely, N-terminal deletion of JRK JRK( $\Delta$ N49) was predominantly observed in the cytoplasm and at the cellular membrane (Figure 4d). The large foci have previously been described as JRK binding to chromosome 15 centromere.<sup>10</sup> However, fluorescence *in situ* hybridization assay using chromosome 15 centromere probe and cell karyotyping of several cancer cell lines show that the localization and number of these large foci are not linked to chromosome 15 (Supplementary Figure 3).

The JRK protein binds to the  $\beta$ -catenin transcriptional machinery and the gene is transcriptionally regulated by TCF7L2

In agreement with a previous report<sup>5</sup> we found JRK in complex with the  $\beta$ -catenin transcriptional machinery including  $\beta$ -catenin itself, TCF7L2 and LEF1 (Figure 5a). Furthermore, we also observed the interaction between  $\beta$ -catenin and JRK using endogenous protein (Figure 5b). Importantly, we found  $\beta$ -catenin N-terminal domain (amino acid 1–217) to be sufficient for binding to

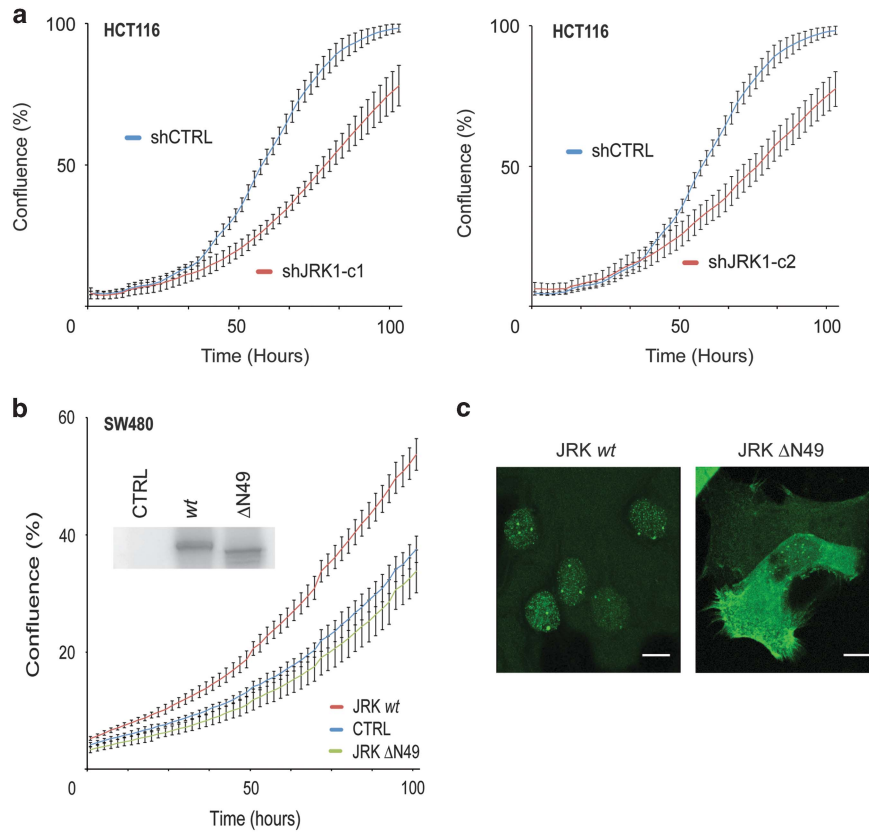


**Figure 4.** The N-terminal domain of JRK is required to promote cell proliferation. **(a)** Loss of JRK expression in HCT116 resulted in a decrease in cell proliferation, compared with control. JRK was stably knocked down in HCT116 using lentivirus. To rule out that the observed reduction in proliferation was a consequence of random shRNA integration, proliferation was assessed using two clones. Data were recorded using Incucyte as an average of three wells per conditions and four reads per well. **(b)** Ectopic stable expression of JRK-WT but not JRK- $\Delta$ N49 increases cell proliferation in SW480 cells. Proliferation of SW480 stably transfected with JRK-WT, JRK- $\Delta$ N49 or vector control (CMV6) were recorded using Incucyte as an average of 3 wells per conditions and four reads per well. **(c)** JRK- $\Delta$ N49 shows a different subcellular localization to JRK-WT. JRK-WT(GFP) or JRK- $\Delta$ N49(GFP) were transfected in HCT15 and their subcellular localization assessed by confocal microscopy.

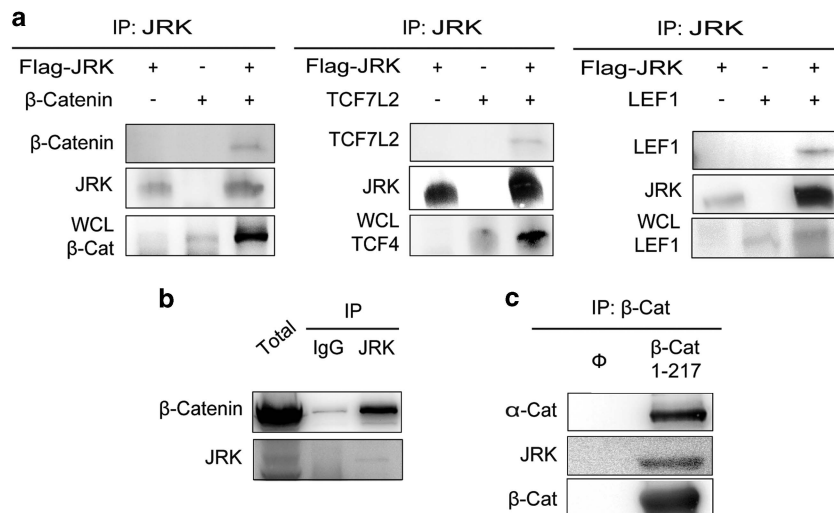


**Figure 5.** JRK binds to the  $\beta$ -catenin transcriptional machinery. **(a)** Co-immunoprecipitation experiments identify JRK in complex with  $\beta$ -catenin, TCF7L2 and LEF1. 293T cells were cotransfected with different expression plasmids as labeled. JRK was immunoprecipitated (IP) with anti-FLAG antibody. Immunoprecipitates were run and the membrane blotted with the appropriate antibody. **(b)** Endogenous JRK interacts with endogenous  $\beta$ -catenin in DLD1 cells. Lysates were immunoprecipitated with JRK or IgG antibodies and blotted with the appropriate antibody. **(c)** JRK binds to  $\beta$ -catenin N-terminal region (amino acids 1–217). 293T cells were transfected with a vector containing the N-terminal domain of  $\beta$ -catenin (amino acids 1–217). N-terminal  $\beta$ -catenin was immunoprecipitated with anti-GFP antibody and the immunoprecipitates were run and blotted with the appropriate antibody. wcl, whole-cell lysate.

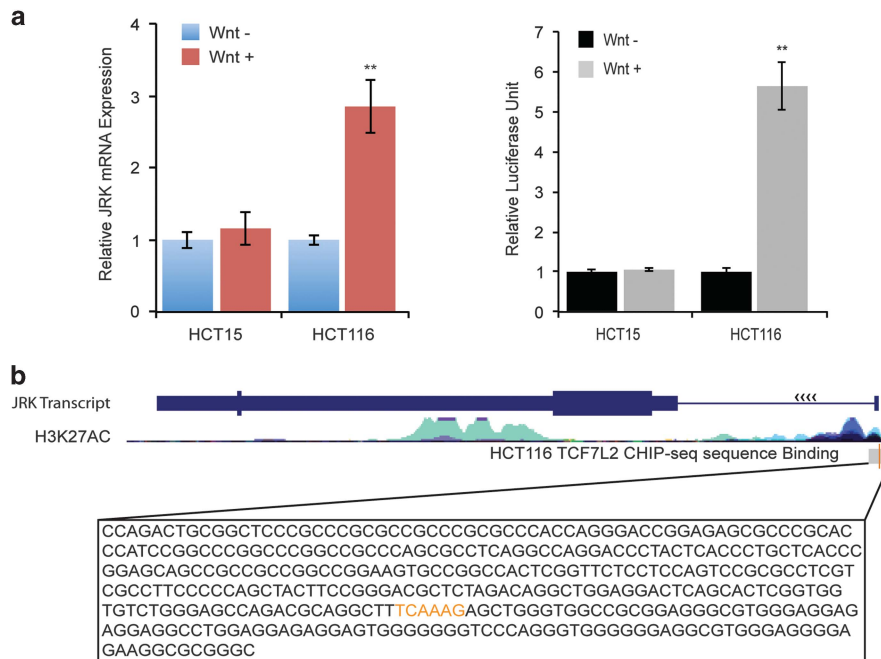


**Figure 6.** JRK is a  $\beta$ -catenin/TCF7L2 target gene. **(a)** JRK expression increases in HCT116 cells following Wnt3a stimulation. HCT15 or HCT116 cell lines were treated with Wnt3a conditioned media or mock treated for 24 h. RNA was extracted and JRK expression was assessed by qPCR. Wnt3a activates  $\beta$ -catenin transcription in HCT116 but not in HCT15 cells. HCT15 or HCT116 cells were transiently transfected with 1  $\mu$ g of the  $\beta$ -cat/TCF/LEF luciferase reporter construct, and  $\beta$ -catenin transcriptional activity was measured by the TOPFlash luciferase assay. The y axis shows normalized relative luciferase activity, data are represented as mean s.d.,  $n = 3$ . **(b)** Chromatin immunoprecipitation sequencing data on HCT116 cell line identifies TCF7L2 binding in proximity to *JRK* transcriptional start site<sup>13</sup> (Figure 6b). Analysis of this chromatin immunoprecipitation sequencing sequence confirms the presence of a TCF7L2 consensus binding site (TCAAAG).

endogenous JRK (Figure 5c). This region of  $\beta$ -catenin has been described as a potential 'targetable' region.<sup>11</sup>

As most  $\beta$ -catenin regulators are themselves regulated by Wnt/ $\beta$ -catenin,<sup>12</sup> we next determined whether *JRK* expression was under  $\beta$ -catenin regulation. Indeed, Wnt stimulation of HCT116 cells induced *JRK* mRNA expression and this was not seen in APC-deficient HCT15 cells (Figure 6a). This finding raises the possibility that *JRK* is a  $\beta$ -catenin/TCF7L2 target gene. Remarkably, whole-genome chromatin immunoprecipitation sequencing analyses performed on HCT116 cell line identified TCF7L2 binding in proximity to *JRK* transcriptional start site<sup>13</sup> (Figure 6b). TCF7L2 consensus binding site has been extensively studied.<sup>14</sup> Detailed analysis of the chromatin immunoprecipitation sequencing sequence confirmed the presence of a TCF7L2 consensus binding site (Figure 6b).

## DISCUSSION

The loss of a number of  $\beta$ -catenin inhibitory components is a well-established mechanism of  $\beta$ -catenin hyperactivation in cancer. On the other hand, fewer oncogenic proteins that promote  $\beta$ -catenin hyperactivity, such as CBP, TCF7L2 or BCL9, have been identified. These proteins are of particular interest as they offer novel therapeutic opportunities to target hyperactive  $\beta$ -catenin activity even for the commonly occurring APC-mutated tumors.

This study brings several lines of evidence to support the protein JRK as a positive regulator of  $\beta$ -catenin with promising therapeutic value; (1) *JRK* is commonly overexpressed in three major cancer types; colon, breast and ovarian. (2) High *JRK* expression, in human colorectal cancer tumors, is significantly associated with an increase in  $\beta$ -catenin target gene expression and nuclear localization. (3) JRK is required for efficient  $\beta$ -catenin transcriptional activity across different cancer cell types, regardless of their APC status. (4) JRK is a core component

of the  $\beta$ -catenin transcriptional complex and several other components of this complex are now actively pursued as promising therapeutic targets such as TCF7L2,<sup>15</sup> BCL9<sup>16</sup> and CBP.<sup>17</sup> (5) JRK binds to the 'targetable' N-terminal  $\beta$ -catenin domain (residues 1–217).<sup>11</sup>

The detailed mechanism by which JRK upregulates  $\beta$ -catenin activity is still unclear. JRK binds to DNA,<sup>18</sup> which raises the possibility that JRK in complex with  $\beta$ -catenin could relocate  $\beta$ -catenin to different genomic locations and thereby directing the transcription of specific target genes. Furthermore, we show that *JRK* is a Wnt-inducible gene indicating that JRK is part of a positive feedback loop, possibly reinforcing the Wnt pathway activity.

In agreement with previous work in *Drosophila*, we identified JRK as a core component of the  $\beta$ -catenin transcriptional complex in human cell lines, binding to  $\beta$ -catenin itself, TCF7L2 and LEF1.<sup>5</sup> Importantly, we found JRK binding to a 'targetable' N-terminal part of  $\beta$ -catenin. Hence, this region of  $\beta$ -catenin is of particular interest, as it does not bind to known inhibitors (such as APC or E-cadherin), and a number of highly promising pharmacologic strategies are actively pursuing ways to target this region to inhibit oncogenic Wnt signaling.<sup>16,19,20</sup> Further work is now needed to determine if these approaches,<sup>16,19</sup> could also be used to block JRK/ $\beta$ -catenin interaction. Finally, the widespread amplification of *JRK* in many cancers, beyond those discussed in this paper, notably prostate, liver and head and neck cancers, support the conclusion that JRK is a positive regulator of  $\beta$ -catenin hyperactivity. Taken together, our data suggests that therapeutic mechanisms disrupting JRK function may have utility in many cancer types, making it a strong candidate target for an umbrella therapeutic trial.

In conclusion, we propose that JRK is a positive regulator of  $\beta$ -catenin hyperactivity and strategies aimed at blocking

JRK/ $\beta$ -catenin interaction could have some therapeutical benefits in cancers with high JRK expression.

## MATERIALS AND METHODS

### Cell culture

All cancer cell lines, RKO, SW480, HCT116, HCT15, MCF7, HCC1500 and TOV112D were propagated as recommended by the American Type Culture Collection and regularly tested for mycoplasma contamination. All cancer cell lines were authenticated by Cell Bank Australia by short tandem repeat profiling, in line with the draft international standard currently being prepared by the ATCC Standards Development Organisation Workgroup ASN-0002 (04 May 2011).

### Antibodies

The following antibodies were used: anti- $\beta$ -catenin (BD Bioscience, Franklin Lakes, NJ, USA, #610153, Abcam, Cambridge, UK, #AB32572), anti-JRK (Santa Cruz Biotechnology, Santa Cruz, CA, USA, #sc-87174, Abcam #H00008629-B01P, Biorbyt, Cambridge, UK, #0rb35995, Sigma Aldrich, St Louis, MO, USA, #sab1406696), anti-LEF1 (Cell Signaling Technology, Danvers, MA, USA, #2230P), anti-TCF4 (TCF7L2; Cell Signaling Technology #2569P), GAPDH (4300, Ambion, Austin, TX, USA), anti-FLAG (Sigma Aldrich #F1804), Horseradish peroxidase-conjugated anti-mouse, or anti-rabbit IgG (GE Healthcare, Amersham, UK).

### Patient samples

The colorectal cancer specimens were resected at the South Western Sydney Area Health Service hospitals 2000–2003, after patients gave informed consent. The study was approved by the Ethics Review Committees of Royal Prince Alfred and Liverpool Hospitals by protocol numbers X08-0224, HREC/08/RPAH/376, LPOOL 2007/035 and HREC/14/RPA/176. Matched tumors and normal tissue were biopsied by an Anatomical Pathologist from the surgery specimen, snap frozen and stored at  $-80^{\circ}\text{C}$ . Immunohistochemistry was performed using tissue microarrays prepared from the matched formalin-fixed paraffin embedded specimens.<sup>21</sup> Staining was performed using DAKO autostainer (Dako, Glostrup, Denmark). DAKO s2367 (pH 9) solution at  $95^{\circ}\text{C}$  was used in antibody retrieval for 20 min. Primary antibody: mouse anti- $\beta$ -catenin (BD Bioscience #610153) 1:1000 for 60 min. Secondary antibody: mouse Envision HRP for 30 min. Slides were scored blindly by two independent researchers, one of whom was a specialist Anatomical Pathologist.

### RNA extraction, cDNA synthesis and quantitative PCR

RNA was extracted from cell lines using the RNeasy Mini kit (Qiagen, Hilden, Germany). RNA was extracted from fresh frozen colorectal cancer patient tissue using the Allprep DNA/RNA/protein Mini kit (Qiagen). RNA concentrations were quantified on the Nanodrop 2000. The Quantitect Reverse Transcription kit (Qiagen) was used for cDNA synthesis, with 700 ng of RNA used per reaction. A negative control reaction, where all components except reverse transcriptase were included in the mix, was carried out for each run.

Taqman qPCR assays (Life Technologies, Scoresby, VIC, Australia) were carried out in the Applied Biosystems 7900HT (Life Technologies), using 2.5  $\mu\text{l}$  of diluted cDNA, 5  $\mu\text{l}$  of Taqman Gene Expression Master Mix (Life Technologies) and 0.5  $\mu\text{l}$  of Taqman assay in a 10  $\mu\text{l}$  reaction mix (*GAPDH*, Hs99999905\_m1; *KCNJ8*, Hs00958961\_m1; *JRK*, Hs00374396\_s1; *LEF1*, Hs01547250\_m1; *MYC*, Hs00153408\_m1; *NKD1*, Hs00263894\_m1; *SOX9*, Hs01001343\_g1; *TNFRSF19*, Hs00218634\_m1; *VEGFA*, Hs01031688\_m1; *AXIN2*, Hs00610344\_m1; *CYCLIND1*, Hs00277039\_m1). All qPCR reactions were carried out in triplicate, with GAPDH used as the housekeeping control gene; the reverse transcription negative control and a no template control were included in each run. The cycling conditions were as follows: 2 min at  $50^{\circ}\text{C}$  then 10 min at  $95^{\circ}\text{C}$ , followed by 40 cycles of denaturation at  $95^{\circ}\text{C}$  for 15 s and annealing/extension at  $60^{\circ}\text{C}$  for 60 s.

The  $\Delta\text{Ct}$  method was used to analyze the qPCR data. Briefly, the mean Ct value of the triplicates of each sample for each gene of interest was calculated, then the mean GAPDH Ct value for each sample was subtracted from this to obtain a  $\Delta\text{Ct}$  value. The formula  $2^{-\Delta\text{Ct}}$  was used to transform the  $\Delta\text{Ct}$  value into the relative gene expression value. The fold change in gene expression was then calculated by dividing the expression of the test sample by the expression of the control sample (that is, in the case of the

patient samples this would be each individual tumor sample normalized to the corresponding matched normal sample).

### Knockdown, proliferation and site directed mutagenesis

JRK shRNA were purchased from Sigma (pMission TRCN0000147500, TRCN0000219822) and JRK siRNA duplexes and nontargeting siRNA from Origene (Rockville, MD, USA, SR305667). Transfections were performed twice, 24 h apart, with 10 nM siRNA using DharmaFECT1 reagent according to the manufacturer's instructions. Cells were harvested or fixed 72 h after the first transfection. The empty pCMV6 vector, pCMV6 containing full-length JRK cDNA (NM\_001077527, Origene) or JRK mutants were transfected using Lipofectamine2000 (Invitrogen, Carlsbad, CA, USA). Site-directed mutagenesis was carried out as previously described.<sup>22</sup>

Live cultures were analyzed using time lapse phase-contrast microscopy at  $37^{\circ}\text{C}$  with the automated Live Cell Imaging System IncuCyte zoom40061 FLR (Essen Bioscience Inc., Ann Arbor, MI, USA). A total of  $2 \times 10^4$  cells per well were seeded triplicate in a 24-well plate, which was immediately loaded into the IncuCyte imaging system. Four images per well were collected at 2 h intervals. The percent confluence of the live cultures was calculated using the IncuCyte software (Essen Bioscience Inc.). Briefly, average confluence was calculated using individual data from each of the four images taken per well at each time point. The data points represent the mean of three wells ( $\pm$  s.e.m.).

### $\beta$ -Catenin TCF/LEF luciferase assay

Exponentially growing cells in 6-well plates were transfected with either the  $\beta$ -cat/TCF/LEF luciferase reporter construct alone (M50 Super 8X TOPFlash), the negative control construct alone (M51 Super 8X FOPFlash) or cotransfected with the indicated JRK plasmid using Xtreme Gene transfection reagent (Roche, Mannheim, Germany). Luciferase reporter plasmids TOPFlash and FOPFlash were gifts from Randall Moon, University of Washington, USA.<sup>23</sup> The beta-galactosidase construct was cotransfected as a normalization control. After an overnight incubation, the cells were stimulated with either control or Wnt3a-conditioned medium, harvested and lysed in Tropix Galacto-Star lysis solution (Applied Biosystems, Life Technologies, T2071). A total of 10  $\mu\text{l}$  of each lysate was incubated with luciferase Assay Reagent (Promega, Madison, WI, USA, E1505) and luciferase reporter assays were performed as previously described.<sup>24</sup> The  $\beta$ -cat/TCF/LEF luciferase activity was normalized with the value of the corresponding beta-galactosidase dependent luciferase activity (Applied Biosystems, Life Technologies, T2254, T2239) and the ratio ( $n=3$ , mean  $\pm$  s.d.) was statistically analyzed ( $t$ -test;  $*P < 0.05$  and  $**P < 0.01$ ).

### Immunofluorescence microscopy and FISH

HCT15 cells were cultured as described above on glass coverslips and processed as previously described.<sup>25</sup> Optical sections were analyzed by confocal microscopy on an inverted microscope (DM IRE2, Leica Microsystems, Wetzlar, Germany) using a  $\times 63/1.4$  numerical aperture HC Plan  $\times 10/25$  objective lens (Leica Microsystems). The contrast was adjusted for all images with the same settings. FISH was performed using a chromosome 15 centromere probe labeled in Spectrum Orange (Vysis CEP 15 (D15Z4), Alpha Satellite DNA Order no. 06J36-015, Abbott Laboratories, Abbott Park, IL, USA) and JRK-GFP as previously described.<sup>10</sup>

### Co-immunoprecipitation and western blotting

Immunoprecipitation was performed on whole-cell lysates resuspended in cold lysis buffer (50 mM Tris-HCl (pH 7.4), 150 mM NaCl, 1 mM EDTA and 0.5% Triton X-100) containing protease inhibitors using the appropriate antibody at  $4^{\circ}\text{C}$  overnight. Immunoprecipitates were resolved on 10% SDS-polyacrylamide gel electrophoresis. Proteins were transferred to nitrocellulose (Millipore, Bedford, MA, USA), immunoprobed and detected by enhanced chemiluminescence (Pierce Chemical, Rockford, IL, USA). Western blotting was performed with the same antibodies used for the immunoprecipitation to control for loading.

### CONFLICT OF INTEREST

The authors declare no conflict of interest.

## ACKNOWLEDGEMENTS

We thank the South Western Sydney Colorectal Tissue Bank for the colorectal cancer patient specimens and Dr Christopher Henderson (Liverpool Hospital, Sydney, Australia) for helping with immunohistochemistry scoring.  $\beta$ -Catenin constructs were a gift from A/Prof Beric Henderson (Westmead Institute for Cancer Research, Westmead Millennium Institute, Sydney, Australia). JRK-FLAG and TCF7L2 constructs were a gift from Dr Benchabane (Department of Genetics and the Norris Cotton Cancer Center, Dartmouth Medical School, Hanover, NH, USA). The M50 Super 8x TOPFlash and M51 Super 8x FOPFlash reporter constructs were obtained from Addgene and originally provided by Prof Randall Moon (University of Washington, Seattle, Washington). This work was supported by grants from the National Health and Medical Research Council of Australia (GNT1020406), Cure Cancer Australia/Cancer Australia (1049846), Cancer Institute NSW (13ECF1-46) and Cancer Institute NSW (10CDF232). The contents of the published material are solely the responsibility of the administering institution, participating institutions or individual authors and do not reflect the views of NHMRC.

## REFERENCES

- Polakis P. Wnt signaling and cancer. *Genes Dev* 2000; **14**: 1837–1851.
- Kramps T, Peter O, Brunner E, Nellen D, Froesch B, Chatterjee S *et al*. Wnt/wingless signaling requires BCL9/legless-mediated recruitment of pygopus to the nuclear beta-catenin-TCF complex. *Cell* 2002; **109**: 47–60.
- Mani M, Carrasco DE, Zhang Y, Takada K, Gatt ME, Dutta-Simmons J *et al*. BCL9 promotes tumor progression by conferring enhanced proliferative, metastatic, and angiogenic properties to cancer cells. *Cancer Res* 2009; **69**: 7577–7586.
- Major MB, Roberts BS, Berndt JD, Marine S, Anastas J, Chung N *et al*. New regulators of Wnt/beta-catenin signaling revealed by integrative molecular screening. *Sci Signal* 2008; **1**: ra12.
- Benchabane H, Xin N, Tian A, Hafler BP, Nguyen K, Ahmed A *et al*. Jerky/Earthbound facilitates cell-specific Wnt/Wingless signalling by modulating beta-catenin-TCF activity. *EMBO J* 2011; **30**: 1444–1458.
- Moore T, Hecquet S, McLellann A, Ville D, Grid D, Picard F *et al*. Polymorphism analysis of JRK/JH8, the human homologue of mouse jerky, and description of a rare mutation in a case of CAE evolving to JME. *Epilepsy Res* 2001; **46**: 157–167.
- Gao J, Aksoy BA, Dogrusoz U, Dresdner G, Gross B, Sumer SO *et al*. Integrative analysis of complex cancer genomics and clinical profiles using the cBioPortal. *Sci Signal* 2013; **6**: pl1.
- Cerami E, Gao J, Dogrusoz U, Gross BE, Sumer SO, Aksoy BA *et al*. The cBio cancer genomics portal: an open platform for exploring multidimensional cancer genomics data. *Cancer Discov* 2012; **2**: 401–404.
- Beroukhi R, Mermel CH, Porter D, Wei G, Raychaudhuri S, Donovan J *et al*. The landscape of somatic copy-number alteration across human cancers. *Nature* 2010; **463**: 899–905.
- Waldron R, Moore T. Complex regulation and nuclear localization of JRK protein. *Biochem Soc Trans* 2004; **32**: 920–923.
- Polakis P. Drugging Wnt signalling in cancer. *EMBO J* 2012; **31**: 2737–2746.
- de la Roche M, Worm J, Bienz M. The function of BCL9 in Wnt/beta-catenin signaling and colorectal cancer cells. *BMC Cancer* 2008; **8**: 199.
- Bernstein BE, Birney E, Dunham I, Green ED, Gunter C, Snyder M. An integrated encyclopedia of DNA elements in the human genome. *Nature* 2012; **489**: 57–74.
- Hatzis P, van der Flier LG, van Driel MA, Guryev V, Nielsen F, Denissov S *et al*. Genome-wide pattern of TCF7L2/TCF4 chromatin occupancy in colorectal cancer cells. *Mol Cell Biol* 2008; **28**: 2732–2744.
- Trosset JY, Dalvit C, Knapp S, Fasolini M, Veronesi M, Mantegani S *et al*. Inhibition of protein-protein interactions: the discovery of druglike beta-catenin inhibitors by combining virtual and biophysical screening. *Proteins* 2006; **64**: 60–67.
- de la Roche M, Rutherford TJ, Gupta D, Veprintsev DB, Saxty B, Freund SM *et al*. An intrinsically labile alpha-helix abutting the BCL9-binding site of beta-catenin is required for its inhibition by carnosic acid. *Nat Commun* 2012; **3**: 680.
- Emami KH, Nguyen C, Ma H, Kim DH, Jeong KW, Eguchi M *et al*. A small molecule inhibitor of beta-catenin/CREB-binding protein transcription [corrected]. *Proc Natl Acad Sci USA* 2004; **101**: 12682–12687.
- Donovan GP, Harden C, Gal J, Ho L, Sibille E, Trifiletti R *et al*. Sensitivity to jerky gene dosage underlies epileptic seizures in mice. *J Neurosci* 1997; **17**: 4562–4569.
- Takada K, Zhu D, Bird GH, Sukhdeo K, Zhao JJ, Mani M *et al*. Targeted disruption of the BCL9/beta-catenin complex inhibits oncogenic Wnt signaling. *Sci Transl Med* 2012; **4**: 148ra17.
- Kawamoto SA, Coleska A, Ran X, Yi H, Yang CY, Wang S. Design of triazole-stapled BCL9 alpha-helical peptides to target the beta-catenin/B-cell CLL/lymphoma 9 (BCL9) protein-protein interaction. *J Med Chem* 2012; **55**: 1137–1146.
- Al-Sohaily S, Henderson C, Selinger C, Pangon L, Segelov E, Kohonen-Corish M *et al*. Loss of special AT-rich sequence-binding protein 1 (SATB1) predicts poor survival in patients with colorectal cancer. *Histopathology* 2014; **65**: 155–163.
- Morris JR, Pangon L, Boutell C, Katagiri T, Keep NH, Solomon E. Genetic analysis of BRCA1 ubiquitin ligase activity and its relationship to breast cancer susceptibility. *Hum Mol Genet* 2006; **15**: 599–606.
- Veeman MT, Slusarski DC, Kaykas A, Louie SH, Moon RT. Zebrafish prickle, a modulator of noncanonical Wnt/Fz signaling, regulates gastrulation movements. *Curr Biol* 2003; **13**: 680–685.
- Pangon L, Mladenova D, Watkins L, Van Kralingen C, Currey N, Al-Sohaily S *et al*. MCC inhibits beta-catenin transcriptional activity by sequestering DBC1 in the cytoplasm. *Int J Cancer* 2014; **36**: 55–64.
- Pangon L, Van Kralingen C, Abas M, Daly RJ, Musgrove EA, Kohonen-Corish MR. The PDZ-binding motif of MCC is phosphorylated at position -1 and controls lamellipodia formation in colon epithelial cells. *Biochim Biophys Acta* 2012; **1823**: 1058–1067.
- Cancer Genome Atlas Network. Comprehensive molecular characterization of human colon and rectal cancer. *Nature* 2012; **487**: 330–337.
- Cancer Genome Atlas Network. Comprehensive molecular portraits of human breast tumours. *Nature* 2012; **490**: 61–70.
- Cancer Genome Atlas Research Network. Integrated genomic analyses of ovarian carcinoma. *Nature* 2011; **474**: 609–615.

Supplementary Information accompanies this paper on the Oncogene website (<http://www.nature.com/onc>)